Acta Materia Medica

Research Article

Discovery and characterization of naturally occurring chalcones as potent inhibitors of bile salt hydrolases

Graphical abstract

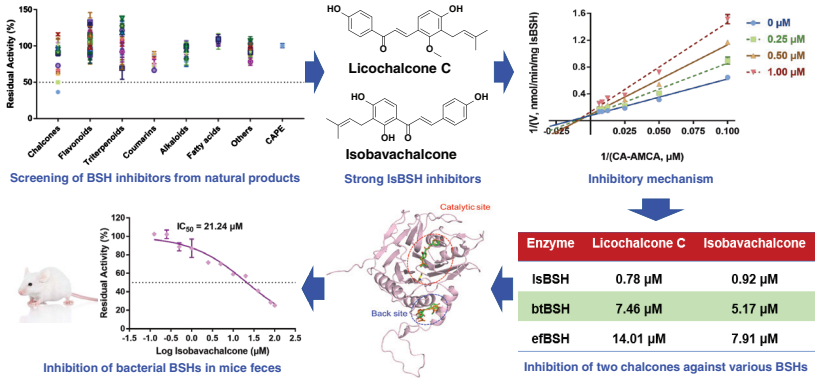

Highlights

- The inhibitory potentials of more than 100 natural compounds against lsBSH are assayed.
- Licochalcone C and isobavachalcone display potent lsBSH inhibitory activity (IC_{50} < 1 μM).
- Licochalcone C and isobavachalcone act as mixed inhibitors of lsBSH.
- Licochalcone C and isobavachalcone inhibit three various BSHs and reduce the total BSH activities in mouse feces.

Authors

Chun-Yu Li, Hao-Nan Wang, Guang-Hao Zhu, Li-Lin Song, Xu-Dong Hou, Peng-Chao Huo, Jie Hou and Guang-Bo Ge

Correspondence

geguangbo@dicp.ac.cn (G. B. Ge); houjie@dmu.edu.cn (J. Hou)

In brief

Licochalcone C and isobavachalcone are naturally occurring inhibitors of BSHs. These two agents can be used as promising lead compounds to develop more efficacious BSH inhibitors for modulating bile acid metabolism

https://doi.org/10.15212/AMM-2022-0003
164 Acta Materia Medica 2022, Volume 1, Issue 2, p. 164-176

compuscript

Acta Materia Medica

Research Article

Discovery and characterization of naturally occurring chalcones as potent inhibitors of bile salt hydrolases

Chun-Yu Li[a], Hao-Nan Wang[a], Guang-Hao Zhu[a], Li-Lin Song[a,b], Xu-Dong Hou[c], Peng-Chao Huo[a], Jie Hou[c,*] and Guang-Bo Ge[a,*]

[a]Shanghai Frontiers Science Center for Chinese Medicine Chemical Biology, Institute of Interdisciplinary Integrative Medicine Research, Shanghai University of Traditional Chinese Medicine, 1200 Cailun Road, Shanghai 201203, China
[b]Dalian Institute of Chemical Physics, Chinese Academy of Sciences, Dalian 116000, China
[c]College of Basic Medical Sciences, Dalian Medical University, Dalian 116044, China

***Correspondence:** geguangbo@dicp.ac.cn (G. B. Ge); houjie@dmu.edu.cn (J. Hou)

Received: 25 January 2022; Revised: 04 April 2022; Accepted: 12 April 2022

Published online: 06 May 2022

DOI: 10.15212/AMM-2022-0003

ABSTRACT

Bile salt hydrolases (BSHs) play crucial roles in the deconjugation of conjugated bile acids and therefore are key targets for modulating bile acid metabolism. This study aimed to identify efficacious BSH inhibitors from a natural compound library and to characterize their inhibitory mechanisms. The inhibitory potential of more than 100 natural compounds against BSH produced by *Lactobacillus salivarius* (lsBSH) was assayed, and several chalcones with strong or moderate lsBSH inhibitory activity were identified. Of all tested chalcones, licochalcone C and isobavachalcone showed the most potent lsBSH inhibitory activity (IC_{50} < 1 μM). Inhibition kinetic analyses demonstrated that both licochalcone C and isobavachalcone reversibly inhibited lsBSH-catalyzed CA-AMCA hydrolysis *via* a mixed manner. Docking simulations suggested that they bind lsBSH at two distinct sites mainly *via* hydrogen bonding and hydrophobic interactions. Additionally, licochalcone C and isobavachalcone were found to inhibit various BSHs and decrease the total BSH activity in mouse feces, thus suggesting that these agents are broad-spectrum BSH inhibitors. Collectively, our findings revealed that licochalcone C and isobavachalcone are naturally occurring inhibitors of BSH, which may serve as promising lead compounds in the development of more efficacious BSH inhibitors for modulating bile acid metabolism.

Keywords: bile salt hydrolases (BSHs), inhibitor, licochalcone C, isobavachalcone, inhibitory mechanism

1. INTRODUCTION

The gut microbiome encodes many enzymes with crucial roles in the biotransformation of diverse xenobiotics and endogenous substances [1]. Among the reported gut-microbiota-produced enzymes in mammals, bile salt hydrolases (BSHs; E. C.3.5.1.24), a group of cysteine hydrolases, are essential in deconjugation of the glycine- or taurine-conjugated bile acids (BAs) [2, 3], *via* catalyzing hydrolytic reactions of the C24 amide bond of conjugated BAs into unconjugated BAs and free glycine or taurine. BAs are key endogenous substances in humans, which have many important biological functions, such as facilitating the digestion and absorption of dietary lipids, as well as acting as hormones or signaling molecules targeting distinct receptors [4-6]. Parts of BAs have been reported to be potent ligands for a range of host nuclear receptors (such as farnesoid X receptor and pregnane X receptor) [7] and G protein-coupled receptors [8], thereby strongly influencing host lipid and glucose metabolic and immunomodulatory processes [9, 10]. Accumulating evidence indicates that BSH abundance and activity are tightly associated with BAs homeostasis and a variety of human diseases including inflammatory bowel disease, obesity, type 2 diabetes, and liver and cardiovascular diseases [11-14], thus suggesting that BSHs are key targets for treating metabolic diseases.

Although multiple natural and synthetic compounds have been found to have BSH inhibitory activity in the past few decades, very few compounds have been reported to have potent inhibition and good safety profiles [15, 16]. Therefore, discovering more effective BSH inhibitors is urgently needed. Given that natural

products remain the major source for the identification of drug leading compounds, we initiated large-scale screening to assess the inhibitory potential of natural products toward lsBSH. After preliminary assessment of six classes of natural products (more than 100 natural products), we identified several naturally occurring chalcones with strong to moderate lsBSH inhibition activity (**Figure 1**). Chalcones are widely found in many medicinal plants and herbs [17, 18], which have been reported to have diverse biological activities, such as anti-inflammatory effects and inhibitory activity against enzymes including tyrosine kinase, aldose reductase, cyclooxygenase, carboxylesterases and pancreatic lipase [19-23]. However, the BSH inhibition activity of naturally occurring chalcones and their inhibitory mechanisms have not been reported and investigated.

The objectives of this study were to determine the inhibitory activity of naturally occurring chalcones on BSH in *vitro* and to investigate the inhibitory mechanisms of two newly identified potent inhibitors of lsBSH. To this end, a series of inhibition assays were first performed to assess the inhibitory potential of chalcones on lsBSH, and the inhibitory mechanisms of licochalcone C and isobavachalcone (two most potent inhibitors against lsBSH) were investigated in detail through a range of inhibition kinetic assays, fluorescence quenching assays and docking simulations. These findings should advance medicinal chemists' understanding of the inhibitory mechanisms of chalcones against bacterial BSHs and support the development of more efficacious BSH inhibitors for modulating BA metabolism.

2. MATERIALS AND METHODS

2.1 Chemicals and reagents

Licochalcone A, licochalcone B, licochalcone C and licochalcone D were purchased from Vikeqi Biology Technology Co., Ltd. (Sichuan, China). Naringenin chalcone, flavokawain A, 4′-*O*-methylbroussochalcone B and taurocholic acid (TCA) were ordered from Yuanye Bio-Technology Co., Ltd. (Shanghai, China). Butein and dithiothreitol (DTT) were ordered from J&K Chemical Ltd. (Beijing, China). Caffeic acid phenethyl ester (CAPE) was ordered from Dalian Meilun Biotech Co., Ltd. (Dalian, China). Isoliquiritigenin, echinatin, isobavachalcone, bavachalcone, isoliquiritin, neoisoliquiritin and other natural compounds used in BSH inhibition assays were obtained from Chengdu Pufei De Biotech Co., Ltd. (Chengdu, China), and 2′,4′-Dihydroxy-6′-methoxy-3′,5′-dimethylchalcone was provided by Mr. Wei Xing of East China University of Science and Technology. The purity of all tested natural compounds exceeded 98%. Glycerol, imidazole, sodium acetate, NaCl, lysozyme and phenylmethylsulfonyl fluoride were ordered from Sinopharm Chemical Reagent Co., Ltd. SuperNuclease was obtained from Sino Biological Inc. The cholic acid-AMCA probe (CA-AMCA) was synthesized by author Peng-chao Huo, whereas its hydrolytic metabolite 7-amino-4-methyl-3-coumarinylacetic acid (AMCA) was provided by Energy Chemical Ltd. (Shanghai, China). LC grade methanol, acetonitrile, DMSO and formic acid were ordered from Tedia (Fairfield, OH, USA) and used carefully, and 100 mM phosphate buffered saline (PBS, pH 6.0) was prepared with ultrapure water.

2.2 Expression and purification of BSHs

Expression constructs for amino-terminally fused BSHs (lsBSH, btBSH or efBSH) in a pET29a (+) vector were overexpressed in *Escherichia coli* (*E. coli*) [14, 24, 25]. The expression plasmid was transformed into BL21 (DE3) cells, and expression was induced through the auto-induction method at 18°C. After 36 h of induction, cells were harvested by centrifugation and resuspended in 40 mL lysis buffer (25 mM Tris-HCl, pH 8.0, mixed with 150 mM NaCl, 1 mM DTT, 1 mM phenylmethylsulfonyl fluoride, 0.1 mg/mL lysozyme and 25 U/mL SuperNuclease). After 30 min at room temperature, the cells were lysed

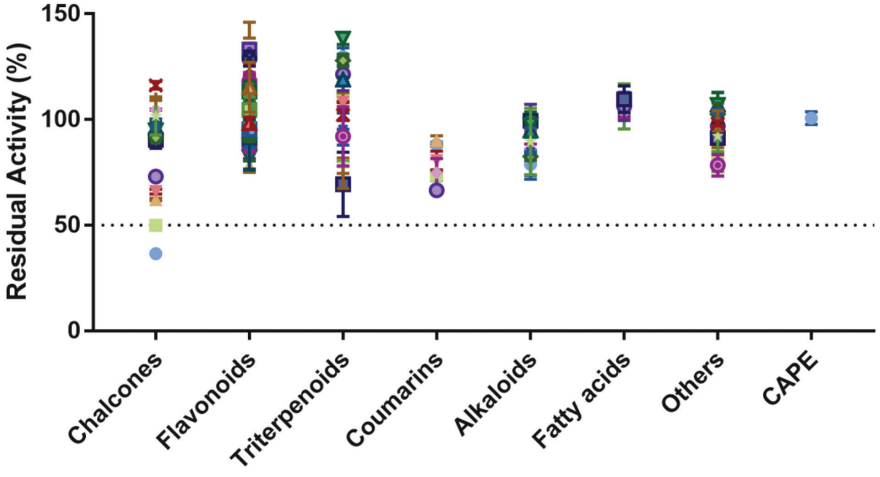

Figure 1 | Inhibitory effects of more than 100 types of natural products (1 μM final concentration) on lsBSH. All data are shown as mean ± SD of triplicate determinations.

Acta Materia Medica

by sonication on ice and centrifuged at 18000 rpm at 4°C for 30 min. Subsequently, 2 mL Ni-NTA agarose was mixed with supernatant, and the lsBSHs was eluted with elution buffer (25 mM Tris-HCl, pH 8.0, 150 mM NaCl, 1 mM DTT and 100–200 mM imidazole). The eluted protein was purified on a Superdex 200 10/300 GL column equilibrated in protein storage buffer (10 mM sodium acetate, pH 5.5, 400 mM NaCl and 1 mM DTT) (**Figure S1**).

2.3 Chemical synthesis of CA-AMCA

CA-AMCA was synthesized according to a published method (**Figure S2**) [26]. Both ^{1}H- and ^{13}C-NMR spectra were used for structural characterization of CA-AMCA, which were acquired on a Bruker AVANCE instrument, with DMSO-d6 as the solvent. Chemical shifts were recorded by using tetramethylsilane as the reference. ^{1}H NMR (600 MHz, DMSO-d6) δ (ppm): 10.34 (s, 1H), 7.91–7.64 (m, 2H), 7.49 (dd, *J* = 8.8, 2.1 Hz, 1H), 4.33 (s, 1H), 4.13 (s, 1H), 4.06–3.95 (m, 1H), 3.80 (s, 1H), 3.62 (s, 1H), 3.53 (d, *J* = 18.0 Hz, 2H), 3.19 (dt, *J* = 11.0, 6.3 Hz, 1H), 2.41 (ddd, *J* = 14.7, 10.1, 4.6 Hz, 1H), 2.36 (s, 3H), 2.32–2.11 (m, 3H), 2.05–1.94 (m, 1H), 1.91 (s, 1H), 1.89–1.71 (m, 5H), 1.71–1.60 (m, 2H), 1.51–1.41 (m, 3H), 1.41–1.15 (m, 7H), 1.03–0.93 (m, 4H), 0.81 (s, 3H), 0.60 (s, 3H). ^{13}C NMR (150 MHz, DMSO-d6) δ (ppm): 173.02, 161.43, 152.76, 148.82, 142.53, 126.41, 115.61, 115.59, 105.64, 71.47, 70.90, 66.70, 46.55, 46.22, 41.98, 41.85, 40.52, 35.78, 35.62, 35.37, 34.86, 34.04, 31.70, 30.87, 29.05, 27.75, 26.69, 23.29, 23.10, 21.64, 17.64, 15.37, 12.83. ESI-MS m/z: 624.35 $[M+H]^+$ (**Figures S3–S5**).

2.4 LC-FD analysis of CA-AMCA and its hydrolytic product AMCA

Both CA-AMCA and AMCA were analyzed with an LC system equipped with a RF-20A fluorescence detector (Shimadzu, Kyoto, Japan) (**Figure S6**). Chromatographic separation was performed on a Shim-pack VP-ODS C18 column (4.6 mm × 150 mm, 5 mm, Shimadzu, Japan), and the column temperature was kept at 40 ˚C. The fluorescence signals of AMCA and CA-AMCA were recorded with an excitation wavelength at 345 nm and emission wavelength at 455 nm. The mobile phase was a mixture of acetonitrile (A) and 0.2% formic acid water (B) with the following gradient conditions: 0–2 min, 75%–55% B; 2–3 min, 55%–20% B; 3–5 min, 20%–10% B; 5–5.1 min, 10%–75% B; and 5.1–7 min, maintenance at 75% B. The flow rate was 0.5 mL/min. The standard curve for AMCA and an enzymatic kinetic plot of lsBSH-catalyzed CA-AMCA hydrolysis are shown in **Figures S7** and **S8**, respectively.

2.5 BSHs inhibition assays using CA-AMCA as a substrate

Briefly, a mixture (190 μL) containing lsBSH (2 μg/mL final concentration), DTT (1 mM final concentration) and various inhibitors was pre-incubated in 100 mM PBS (pH 6.0) at 37°C for 3 min. Subsequently, 10 μL reaction buffer containing 0.2 mM CA-AMCA was added to start the biotransformation. The reaction was terminated with ice-cold acetonitrile (200 μL) after incubation at 37°C for 30 min. After centrifugation at 20000 × g for 30 min, 100 μL of the supernatant was transferred into an LC vial and analyzed with LC-FD. The residual activity of BSH was calculated as: (peak area of AMCA in the presence of inhibitor)/peak area of AMCA in negative control (DMSO only) × 100%.

2.6 Inhibition of TCA hydrolysis by licochalcone C and isobavachalcone

In brief, a mixture (190 μL) containing lsBSH (2 μg/mL), DTT (1 mM) and various inhibitors was pre-incubated in 100 mM PBS (pH 6.0) at 37°C for 3 min. Subsequently, 10 μL of PBS containing 1 mM TCA was added to start the biotransformation. The reaction was terminated with ice-cold acetonitrile (200 μL) containing the internal standard diclofenac after incubation at 37°C for 30 min. Then the mixtures were centrifuged at 20000 × g for 30 min, and 100 μL of the supernatant was diluted with 100 μL ultrapure water. The samples were analyzed with LC-MS/MS according to a published method with minor modifications [27].

2.7 Inhibition kinetic analyses of licochalcone C and isobavachalcone

To explore the inhibitory mechanisms of the two natural chalones against lsBSH, we performed a series of inhibition assays with various concentrations of the fluorescent substrate CA-AMCA and increasing concentrations of inhibitors. The inhibition kinetics was determined by the intersection point in the Lineweaver-Burk plot. The slopes of the lines in the Lineweaver-Burk plot were then used to depict the second plot and to determine the inhibition constant (K_i) value [28-30]. The following equations for competitive (a), non-competitive (b) or mixed inhibition (c) were used.

$$V = (V_{max}S) / [K_m(1 + I / K_i) + S] \quad \text{(a)}$$

$$V = (V_{max}S) / [(K_m + S) \times (1 + I / K_i)] \quad \text{(b)}$$

$$V = (V_{max}S) / [(K_m + S) \times (1 + I / \alpha K_i)] \quad \text{(c)}$$

where V is the velocity of CA-AMCA hydrolyzed by lsBSH, and V_{max} is the maximum velocity. S and I are substrate (CA-AMCA) and inhibitor concentrations, respectively. K_i is the inhibition constant of the inhibitors toward lsBSH, and K_m is the Michaelis constant for CA-AMCA hydrolyzed by lsBSH.

2.8 Fluorescence quenching assays

Fluorescence spectra of lsBSH with or without inhibitor were recorded with a Duetta fluorescence and absorption spectrometer (HORIBA Scientific). In brief, 1 mL of 100 mM PBS (pH 6) containing lsBSH (20 μg/mL), TCEP

(0.25 mM) and inhibitors in increasing concentrations (0, 0.25, 0.5, 1, 1.5, 2, 3 and 4 μM) was used. After incubation at 25 ˚C for 10 min, the mixture was transferred to a cuvette and scanned at an excitation wavelength of 274 nm. The fluorescence quenching mechanism was described by the Stern-Volmer equation:

$$F_0 / F = 1 + K_{SV}[Q] = 1 + K_q \tau_0 [Q] \quad \text{(d)}$$

where F_0 and F are the fluorescence intensity in the absence and presence of inhibitors, respectively. K_{SV} is the Stern-Volmer dynamic quenching constant. K_q is the bimolecular fluorescence quenching rate constant. τ_0 is the fluorescence lifetime of the fluorescent group without the quencher, and [Q] is the concentration of inhibitors. For biological macromolecules, the average value of τ_0 was approximately 10^{-8} s.

2.9 Molecular docking simulations

Docking simulations were performed with AutoDock Vina (Version 1.1.2). First, the crystal structure of lsBSH (PDB ID: 5YP7) was obtained from Protein Data Bank (https://www.rcsb.org/). Then the hydrogens were added, and the Kollman charges were assigned. The search space was set to 70 × 70 × 70 ˚C Å^3, centered on the catalytic residue Cys2 with a spacing of 0.375 Å. The docking modes with the lowest binding energy were displayed and further analyzed.

2.10 Inhibition of BSHs in mouse feces by licochalcone C and isobavachalcone

Fecal pellets collected form six healthy ICR mice were suspended in PBS and then broken into fine particles to a final concentration of 50 mg/mL. The mixtures were centrifuged at 9000 × g for 30 min at 4°C, and the supernatants were mixed in equal volumes. The reaction solutions (100 μL) contained the fecal solution (1 mg/mL, final concentration), DTT (1 mM, final concentration), inhibitors in increasing concentrations and CA-AMCA (10 μM, final concentration). The reaction was quenched with ice-cold acetonitrile (300 μL) after incubation at 37°C for 30 min. After centrifugation at 20000 × g for 30 min, 100 μL of the supernatant was transferred into an LC vial and analyzed by LC-FD.

2.11 Statistical analysis

All inhibition assays were conducted in triplicate. All data are shown as the mean ± SD of triplicate determinations. The inhibition data (IC_{50} and K_i values) were evaluated in GraphPad Prism 7.0 software (GraphPad Software, Inc., La Jolla, USA).

3. RESULTS AND DISCUSSION

3.1 Screening of lsBSH inhibitors from a natural-product library

To identify strong BSH inhibitors from natural products, we measured the inhibitory potential of 110 natural compounds against lsBSH at three inhibitor concentrations (1 μM, 10 μM and 100 μM). As presented in Figure 1 and Table S1, several naturally occurring chalcones strongly inhibited lsBSH, and licochalcone C and isobavachalcone showed the greatest inhibition, with more than 50% activity loss at a dose of 1 μM. In contrast, the residual activity of lsBSH in the presence of the other tested compounds, including the positive lsBSH inhibitor (CAPE), exceeded 50% at a dose of 1 μM. This finding encouraged us to further study the inhibitory effects of naturally occurring chalcones against lsBSH and other bacterial BSHs.

3.2 Inhibition on lsBSH-catalyzed CA-AMCA hydrolysis by chalones

Among all tested chalcones, two chalcone glycosides (isoliquiritin and neoisoliquiritin) and flavokawain A (a polymethoxylated chalcone) showed very weak lsBSH inhibitory activity even at a high inhibitor concentration (100 μM). To quantify the inhibitory potency of another 12 natural chalcones, we plotted the dose-response curves with increasing inhibitor concentrations. As shown in Figure 2 and Figure S9, all tested chalcones dose-dependently inhibited lsBSH-catalyzed CA-AMCA hydrolysis. The chemical structures and IC_{50} values of all tested chalcones are listed in Table 1. Of these, licochalcone C and isobavachalcone showed the most effective lsBSH inhibitory activity, with IC_{50} values less than 1 μM. Meanwhile, the inhibitory effects of bavachalcone, 4′-*O*-methylbroussochalcone B, licochalcone D, licochalcone A and 2′,4′-dihydroxy-6′-methoxy-3′,5′-dimethylchalcone were also stronger than that of the positive inhibitor CAPE (IC_{50} = 13.64 μM, Figure S10). Other tested chalcones displayed moderate inhibition, with IC_{50} values ranging from 10 μM to 100 μM. These results clearly suggested that parts of naturally occurring chalcones potently inhibited lsBSH, some of which are more potent than previously reported positive lsBSH inhibitors.

After carefully analyzing the inhibitory effect of these natural chalcones on lsBSH, we summarized the structural-inhibition relationships of chalcones as lsBSH inhibitors. First, the addition of a glucosyl group on the chalcone skeleton was found not to be beneficial for lsBSH inhibition. In contrast, the chalones with multiple hydroxyl groups showed good lsBSH inhibition. When the hydroxyl groups at C-4′, C-6′ and C-4 were replaced by methoxy groups, the inhibition effect was weakened, as evidenced by naringenin chalcone (IC_{50} = 22.42 μM) *vs* flavokawain A (IC_{50} > 100 μM). Moreover, the introduction of an unsaturated alkyl chain in the A or B ring was beneficial for lsBSH inhibition, as evidenced by isobavachalcone (IC_{50} = 0.92 μM), bavachalcone (IC_{50} = 1.15 μM) *vs* isoliquiritigenin (IC_{50} = 14.90 μM), as well as licochalcone C (IC_{50} = 0.78 μM), Licochalcone A (IC_{50} = 3.73 μM) *vs* echinatin (IC_{50} = 33.17 μM). These findings should be very useful for the medicinal chemists in designing and developing more efficacious chalcone-type lsBSH inhibitors.

Acta Materia Medica

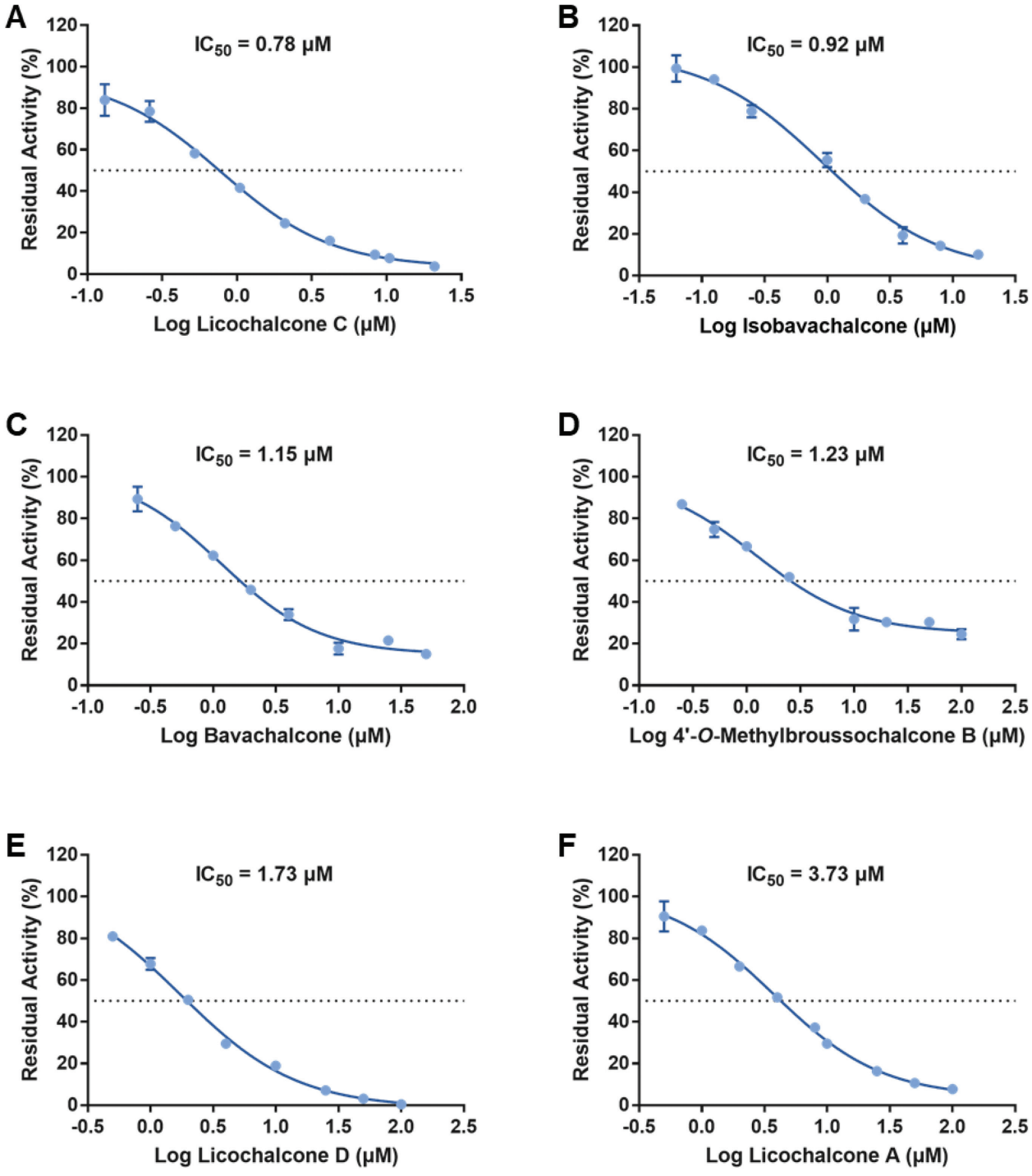

Figure 2 | Dose-inhibition curves of six natural chalcones (IC_{50} < 5 μM) against lsBSH-catalyzed CA-AMCA hydrolysis.
(A) Licochalcone C, (B) isobavachalcone, (C) bavachalcone, (D) 4′-*O*-methylbroussochalcone B, (E) licochalcone D, (F) licochalcone A. All data are shown as mean ± SD of triplicate determinations.

3.3 Inhibition of lsBSH-catalyzed TCA hydrolysis by licochalcone C and isobavachalcone

Given that conjugated BAs are the physiological substrates of lsBSH, we investigated the inhibitory effects of two chalcones on lsBSH-catalyzed TCA hydrolysis. As shown in Figure S11, both licochalcone C and isobavachalcone strongly inhibited lsBSH in a dose-dependent manner, with IC_{50} values of 2.57 μM and 5.84 μM, respectively. These results clearly showed that licochalcone C and isobavachalcone inhibited the hydrolysis of

Table 1 | Chemical structures of chalcones and their IC_{50} values against lsBSH. All data are shown as mean ± SD of triplicate determinations

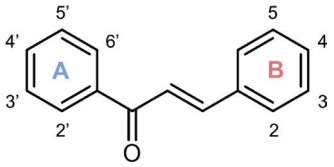

	Name	C2′	C3′	C4′	C5′	C6′	C2	C3	C4	C5	IC_{50} (μM)
1	Isoliquiritigenin	–OH	–H	–OH	–H	–H	–H	–H	–OH	–H	14.90
2	Echinatin	–H	–H	–OH	–H	–H	–OMe	–H	–OH	–H	33.17
3	Naringenin chalcone	–OH	–H	–OH	–H	–OH	–H	–H	–OH	–H	22.42
4	Butein	–OH	–H	–OH	–H	–H	–H	–OH	–OH	–H	17.23
5	Flavokawain A	–OH	–H	–OMe	–H	–OMe	–H	–H	–OMe	–H	>100
6	Isobavachalcone	–OH		–OH	–H	–H	–H	–H	–OH	–H	0.92
7	Bavachalcone	–OH	–H	–OH		–H	–H	–H	–OH	–H	1.15
8	4′-O-Methylbroussochalcone B	–OH	–H	–OMe		–H	–H	–H	–OH	–H	1.23
9	Licochalcone B	–H	–H	–OH	–H	–H	–OMe	–OH	–OH	–H	74.42
10	Licochalcone A	–H	–H	–OH	–H	–H	–OMe	–H	–OH		3.73
11	Licochalcone C	–H	–H	–OH	–H	–H	–OMe		–OH	–H	0.78
12	2′,4′-Dihydroxy-6′-methoxy-3′,5′-dimethylchalcone	–OH	$–CH_3$	–OH	$–CH_3$	–OMe	–H	–H	–H	–H	5.34
13	Licochalcone D	–H		–OH	–H	–H	–OMe	–OH	–OH	–H	1.73
14	Isoliquiritin	–OH	–H	–OH	–H	–H	–H	–H	–Glu	–H	>100
15	Neoisoliquiritin	–OH	–H	–Glu	–H	–H	–H	–H	–OH	–H	>100

both the optical substrates and physiological substrates catalyzed by lsBSH; therefore, these agents may modulate BA metabolism in the gastrointestinal system.

3.4 Inhibitory mechanisms of licochalcone C and isobavachalcone against lsBSH

Next, a series of inhibition kinetic analyses were performed to explore the inhibitory mechanisms of licochalcone C and isobavachalcone against lsBSH-catalyzed CA-AMCA hydrolysis. First, time-dependent inhibition assays indicated that the inhibition tendency and IC_{50} values of licochalcone C and isobavachalcone were not time dependent, thus suggesting that these two agents were reversible inhibitors of lsBSH (**Figure S12**). We then determined the inhibition modes and the inhibition constants (K_i) of these two natural compounds against lsBSH. As shown in **Figure 3**, the Lineweaver-Burk plots of licochalcone C and isobavachalcone against lsBSH-catalyzed CA-AMCA hydrolysis showed that these two compounds strongly inhibited lsBSH *via* mixed inhibition, with K_i values of 0.73 μM and 1.00 μM, for licochalcone C and isobavachalcone, respectively. These findings clearly demonstrated that both licochalcone C and isobavachalcone effectively and reversibly inhibit lsBSH-catalyzed hydrolytic reactions.

3.5 Fluorescence spectroscopy analysis

Fluorescence quenching assays were also performed to study the interactions of licochalcone C and isobavachalcone with lsBSH. As depicted in **Figure 4A** and **B**, the maximum inherent fluorescence emission of lsBSH was observed around 322 nm, whereas the fluorescence intensity of lsBSH significantly decreased with the addition of increasing concentrations of licochalcone C or isobavachalcone. The quenching mechanism was further analyzed according to the Sterne-Volmer plot. As shown in **Figure 4C** and **D**, a good linear relationship between the F_0/F and the concentration of inhibitors was obtained, thus suggesting that both licochalcone C and isobavachalcone quench the intrinsic fluorescence of lsBSH through a single quenching mechanism. The K_{sv} values of licochalcone C and isobavachalcone were calculated as 0.95×10^6 and 0.82×10^6 L/mol, respectively, whereas the K_q values were calculated as 0.95×10^{14} and

Acta Materia Medica

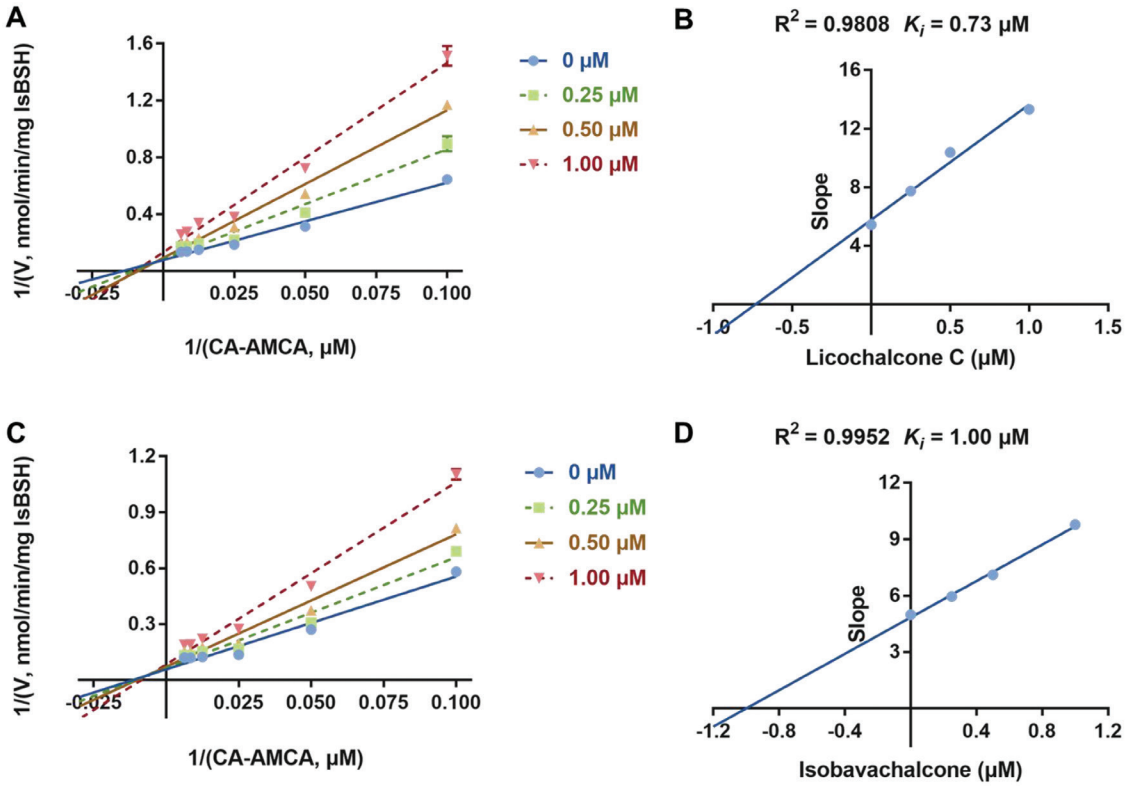

Figure 3 | Lineweaver-Burk plots of licochalcone C (A) and isobavachalcone (C) against lsBSH-catalyzed CA-AMCA hydrolysis. The corresponding second plots show lsBSH inhibition by licochalcone C (B) and isobavachalcone (D).
All data are shown as mean ± SD of triplicate determinations.

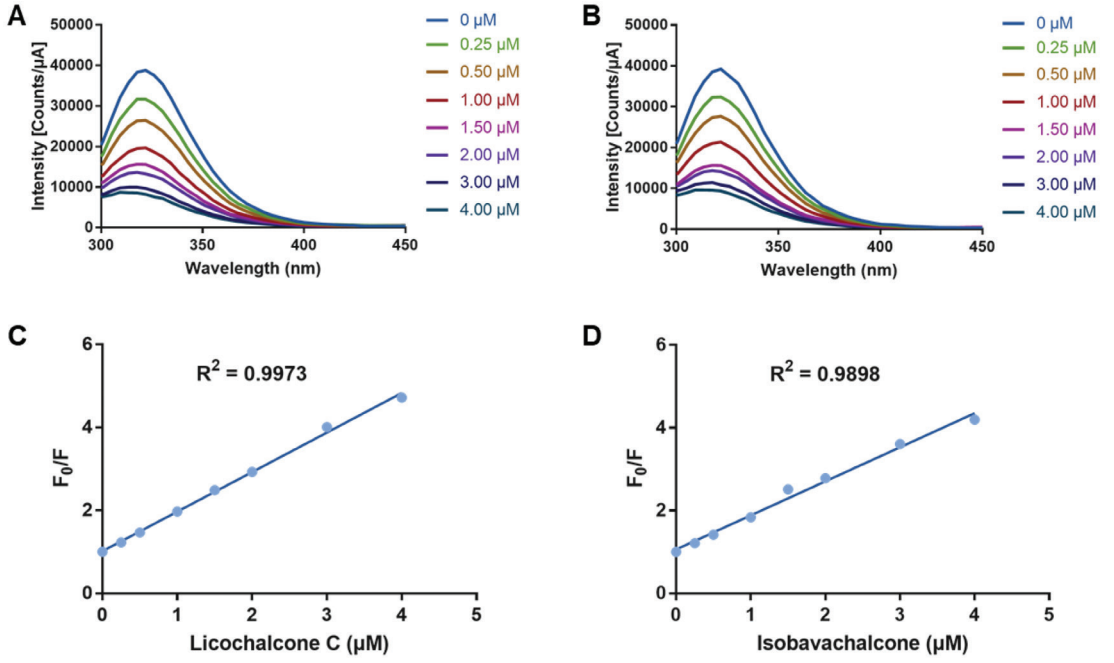

Figure 4 | Fluorescence quenching assays of lsBSH with addition of increasing concentrations of licochalcone C (A) and isobavachalcone (B). The corresponding Stem-Volmer plots for the fluorescence quenching of lsBSH by licochalcone C (C) and isobavachalcone (D) are shown.

0.82 × 10^{14} L/mol/s, respectively. The K_q values of these two agents were much greater than the maximum scatter collision quenching constant of each type of enzyme quencher (2.0 × 10^{10} L/mol/s) [31]. These data indicated that licochalcone C and isobavachalcone quench the intrinsic fluorescence of lsBSH through a static mechanism caused by the formation of ligand-protein complexes, thereby affecting the microenvironment of some important fluorescent groups (such as Trp and Tyr) in lsBSH surrounding the ligand-binding sites.

3.6 Molecular docking simulations

To further investigate the potential ligand-binding sites and the interaction modes between the two newly identified lsBSH inhibitors and the target enzyme, we performed molecular docking simulations of either licochalcone C or isobavachalcone with the reported 3D structure of lsBSH (PDB ID: 5Y7P). Before docking, the potential ligand-binding pockets of lsBSH were predicted with CavityPlus, and the top two potential sites were selected on the basis of ligandability and druggability scores (**Figure S13**). One was located at the catalytic site, which was relatively conserved and contained the key nucleophilic residue Cys2, whereas another was located below the back side of the catalytic site. As shown in **Figure 5**, both licochalcone C and isobavachalcone docked well in the catalytic site or the back site. The spatial conformations of licochalcone C and isobavachalcone superimposed at the catalytic site or the back site are shown in **Figure 5A**. Consequently, the predicted binding energies of both licochalcone C and isobavachalcone on the catalytic site were calculated as –9.3 kcal/mol and –9.4 kcal/mol, respectively, and those on the back site were –6.7 kcal/mol and –7.0 kcal/mol, respectively, thus implying that both agents tightly bound the catalytic site of lsBSH.

At the catalytic site of lsBSH, the benzene rings of the two chalcones formed strong π-π interactions with Phe65 and Phe100, respectively. In addition, licochalcone C strongly interacted with Gly77 and Leu134 *via* hydrogen bonding, whereas isobavachalcone formed a hydrogen bond with Phe130 of lsBSH (**Figure 5B** and **C, Figure S14**). In the back site, two benzene rings of the chalcones formed strong hydrophobic interactions with Leu182 and Phe230, respectively. Meanwhile, a hydrogen bonding interaction between isobavachalcone and Tyr-185 was additionally observed (**Figure 5D** and **E, Figure S15**). These findings clearly indicated that licochalcone C and isobavachalcone stably bind lsBSH at two different ligand-binding sites, thus explaining the mixed inhibition modes of these two agents against lsBSH-catalyzed CA-AMCA hydrolysis. In addition, the interaction of these two agents with Phe and Tyr at each ligand-binding site partly explained the fluorescence quenching effects on the endogenous fluorescence of lsBSH, as shown in the results of the fluorescence quenching assays.

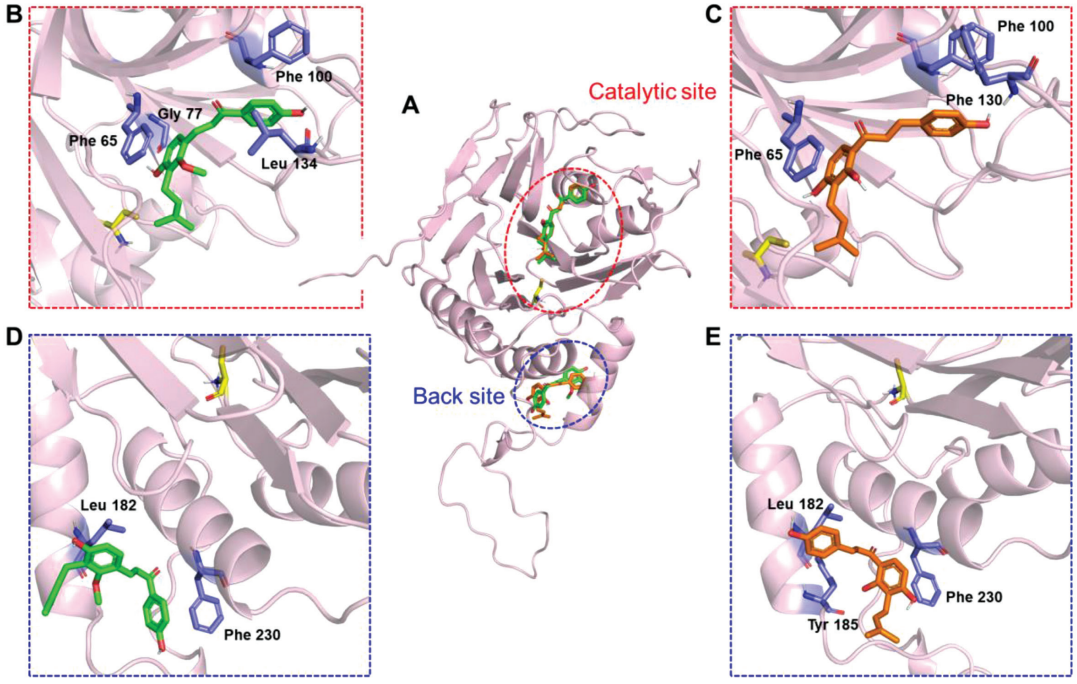

Figure 5 | Stereodiagram of licochalcone C and isobavachalcone superimposed at the catalytic site and the back site (A). The detailed view shows that licochalcone C (green) and isobavachalcone (orange) dock well into the catalytic site (B, C) and back site (D, E) of lsBSH.

The catalytic residue of lsBSH (Cys2) is shown as yellow sticks, and the key residues of lsBSH are shown as blue sticks.

Acta Materia Medica

3.7 Inhibition of licochalcone C and isobavachalcone on other bacterial BSHs

Next, the inhibitory effects of licochalcone C and isobavachalcone on other bacterial BSHs (including btBSH and efBSH) were tested. As shown in Figure 6, both licochalcone C and isobavachalcone inhibited btBSH and efBSH-catalyzed CA-AMCA hydrolysis in a dose-dependent manner. In btBSH, the IC_{50} values of licochalcone C and isobavachalcone were 7.46 μM and 5.17 μM, respectively. In efBSH, the IC_{50} values of these two agents were 14.01 μM and 7.91 μM, respectively. These results demonstrate that these two naturally occurring chalcones inhibit three various bacterial BSHs, thus suggesting that some chalcones can serve as broad-spectrum BSH inhibitors.

3.8 Inhibitory effects of licochalcone C and isobavachalcone against BSHs in mouse feces

Finally, the inhibitory effects of licochalcone C and isobavachalcone on the total activity of bacterial BSHs in mouse feces were evaluated. As shown in Figure 7, both licochalcone C and isobavachalcone blocked the total activity of bacterial BSHs in mouse feces in a dose-dependent manner. The apparent IC_{50} values of these two compounds on the total activity of bacterial BSHs in mouse feces were determined to be 44.66 μM and 21.24 μM, for licochalcone C and isobavachalcone, respectively.

As an important class of signal molecules in the mammals, BAs play a critical role in regulating host metabolism, including energy consumption, glucose and lipid homeostasis, as well as innate and adaptive immune responses [4, 32-34]. BSHs catalyze the critical first step in the metabolism of BAs by microorganisms in the intestinal tract, and their activity significantly influences BA characteristics and many physiological processes in the host [11, 35]. In recent studies, theabrownin from Pu-erh tea has been found to decrease serum and liver cholesterol levels through a mechanism associated with suppression of BSH related microorganisms and BSH activity [36]. In addition, berberine inhibits the activity of BSH in the intestinal flora and significantly increases the level

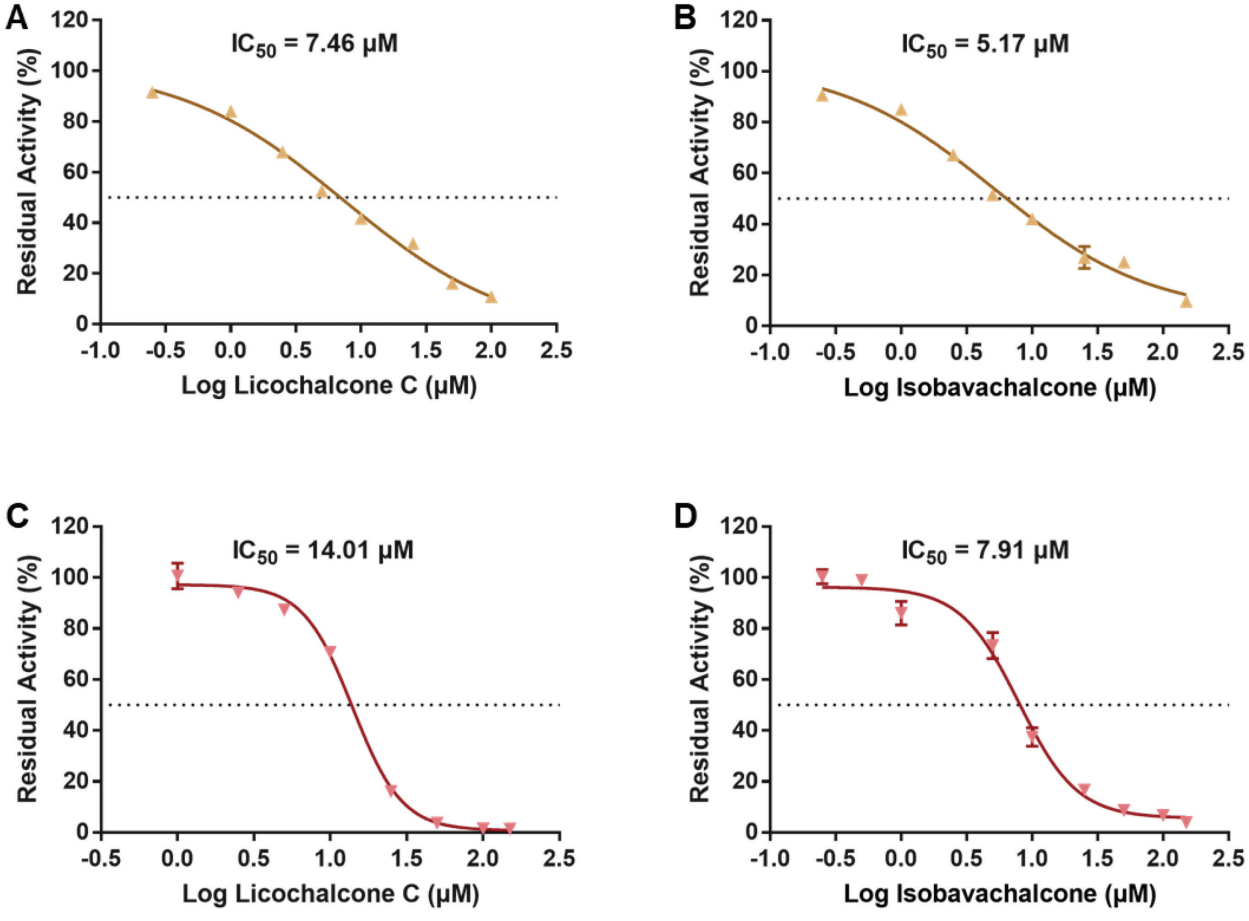

Figure 6 | (A, B) Dose-inhibition curves of licochalcone C and isobavachalcone against btBSH-catalyzed CA-AMCA hydrolysis. (C, D) Dose-inhibition curves of licochalcone C and isobavachalcone against efBSH-catalyzed CA-AMCA hydrolysis.
All data are shown as mean ± SD of triplicate determinations.

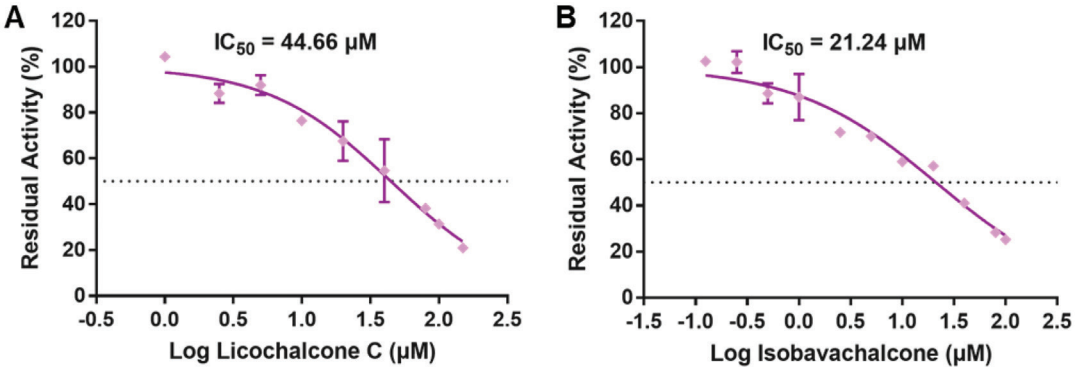

Figure 7 | Dose-inhibition curves of licochalcone C (A) and isobavachalcone (B) against fecal BSH-catalyzed CA-AMCA hydrolysis. All data are shown as mean ± SD of triplicate determinations.

of tauro-cholic acid in the intestines, thereby activating the intestinal FXR pathway and decreasing serum lipid levels [37]. Despite these important implications of BSHs activity, the lack of small-molecule inhibitors has limited deeper study, thus inspiring us to find efficacious BSHs inhibitors from natural products [38].

Chalcones, the intermediates in the biosynthesis of flavonoids, are widely found in medicinal plants such as *Glycyrrhiza inflata* Bat., *Psoralea corylifolia* L. and *Carthamus inctorius* L., and substantially contribute to the medicinal value of these herbs [39-42]. Moreover, these herbs have been shown to modulate BA metabolism [43-45]. In this study, natural chalcones were found to inhibit BSHs strongly or moderately, and these components readily contact BSHs after oral administration of the herbs. Given the low oral bioavailability and rapid hepatic metabolism of natural chalcones, these herbal medicines are highly likely to regulate BA metabolism partly by inhibiting BSHs in intestinal bacteria. Additionally, as a simple scaffold, chalcones can be easily synthesized through several routes, and various of chalcone derivatives have been synthesized and shown enhanced enzyme inhibition, bioavailability or *in vivo* efficacy [19, 46]. Together, these data and findings suggest that medicinal chemists can design and develop more powerful and innovative BSHs inhibitors by using chalcones as a scaffold, aiming to obtain ideal drug candidates for modulating BA metabolism and for treating BA-associated diseases.

4. CONCLUSION

In summary, this study screened the inhibitory potential of more than 100 natural compounds against lsBSH (a key gut-microbiota-produced cysteine hydrolase in deconjugation of conjugated BAs) and indicated that parts of naturally occurring chalcones were strong lsBSH inhibitors. Of all tested compounds, licochalcone C and isobavachalcone showed the most potent inhibitory effects against lsBSH. Further investigation demonstrated that these two naturally occurring chalcones strongly inhibited the lsBSH-catalyzed hydrolytic reaction in a mixed inhibition manner, with K_i values of 0.73 μM and 1.00 μM, respectively. Fluorescence quenching assays suggested that both licochalcone C and isobavachalcone quenched the intrinsic fluorescence of lsBSH through a static mechanism caused by the formation of stable ligand-protein complexes. Molecular docking simulations indicated that both licochalcone C and isobavachalcone stably bind lsBSH at two distinct ligand-binding sites, mainly *via* the formation of hydrogen bonds and hydrophobic interactions. Subsequent studies revealed that these two agents inhibited various bacterial BSHs and the total bacterial BSH activity in mouse feces. These findings demonstrate that licochalcone C and isobavachalcone are strong broad-spectrum BSH inhibitors and suggest that chalcones may be used as lead compounds for developing more efficacious BSH inhibitors.

ACKNOWLEDGEMENTS

This work was supported by the NSF of China (81922070, 81973286), Shanghai Science and Technology Innovation Action Plans (20S21901500, 20S21900900) supported by Shanghai Science and Technology Committee, and Shuguang Program (18SG40), and the Project on the Prevention and Treatment of COVID-19 with Chinese and Western Medicines, supported by Shanghai Education Development Foundation and Shanghai Municipal Education Commission.

CONFLICTS OF INTEREST

No conflicts of interest.

REFERENCES

[1] Koppel N, Balskus EP: Exploring and Understanding the Biochemical Diversity of the Human Microbiota. *Cell Chemical Biology* 2016, 23(1):18-30.

[2] Begley M, Hill C, Gahan CG: Bile Salt Hydrolase Activity in Probiotics. *Applied and Environmental Microbiology* 2006, 72(3):1729-1738.

[3] Ridlon JM, Harris SC, Bhowmik S, Kang DJ, Hylemon PB: Consequences of Bile Salt Biotransformations by Intestinal Bacteria. *Gut Microbes* 2016, 7(1):22-39.

[4] Fiorucci S, Distrutti E: Bile Acid-Activated Receptors, Intestinal Microbiota, and the Treatment of Metabolic Disorders. *Trends Molecular Medicine* 2015, 21(11):702-714.
[5] Martinot E, Sèdes L, Baptissart M, Lobaccaro JM, Caira F, Beaudoin C, et al.: Bile Acids and their Receptors. *Molecular Aspects of Medicine* 2017, 56:2-9.
[6] Macierzanka A, Torcello-Gómez A, Jungnickel C, Maldonado-Valderrama J: Bile Salts in Digestion and Transport of Lipids. *Advances in Colloid and Interface Science* 2019, 274:102045.
[7] Chiang JY: Bile Acid Metabolism and Signaling. *Comprehensive Physiology* 2013, 3(3):1191-1212.
[8] Katsuma S, Hirasawa A, Tsujimoto G: Bile Acids Promote Glucagon-Like Peptide-1 Secretion Through TGR5 in a Murine Enteroendocrine Cell Line STC-1. *Biochemical and Biophysical Research Communications* 2005, 329(1):386-390.
[9] Schaap FG, Trauner M, Jansen PL: Bile Acid Receptors as Targets for Drug Development. *Nature Reviews Gastroenterology & Hepatology* 2014, 11(1):55-67.
[10] Shen H, Ding L, Baig M, Tian J, Wang Y, Huang W: Improving Glucose and Lipids Metabolism: Drug Development Based on Bile Acid Related Targets. *Cell Stress* 2021, 5(1):1-18.
[11] Foley MH, O'Flaherty S, Barrangou R, Theriot CM: Bile Salt Hydrolases: Gatekeepers of Bile Acid Metabolism and Host-Microbiome Crosstalk in the Gastrointestinal Tract. *PLOS Pathogens* 2019, 15(3):e1007581.
[12] Song Z, Cai Y, Lao X, Wang X, Lin X, Cui Y, et al.: Taxonomic Profiling and Populational Patterns of Bacterial Bile Salt Hydrolase (BSH) Genes Based on Worldwide Human Gut Microbiome. *Microbiome* 2019, 7(1):9.
[13] Jia B, Park D, Hahn Y, Jeon CO: Metagenomic Analysis of the Human Microbiome Reveals the Association Between the Abundance of Gut Bile Salt Hydrolases and Host Health. *Gut Microbes* 2020, 11(5):1300-1313.
[14] Yao L, Seaton SC, Ndousse-Fetter S, Adhikari AA, DiBenedetto N, Mina AI, et al.: A Selective Gut Bacterial Bile Salt Hydrolase Alters Host Metabolism. *Elife* 2018, 7:e37182.
[15] Smith K, Zeng X, Lin J: Discovery of Bile Salt Hydrolase Inhibitors Using An Efficient High-Throughput Screening System. *PLoS One* 2014, 9(1):e85344.
[16] Adhikari AA, Seegar TCM, Ficarro SB, McCurry MD, Ramachandran D, Yao L, et al.: Development of A Covalent Inhibitor of Gut Bacterial Bile Salt Hydrolases. *Nature Chemical Biology* 2020, 16(3):318-326.
[17] Asl MN, Hosseinzadeh H: Review of Pharmacological Effects of Glycyrrhiza sp. and Its Bioactive Compounds. *Phytotherapy Research* 2008, 22(6):709-724.
[18] Rudrapal M, Khan J, Dukhyil AAB, Alarousy R, Attah EI, Sharma T, et al.: Chalcone Scaffolds, Bioprecursors of Flavonoids: Chemistry, Bioactivities, and Pharmacokinetics. *Molecules* 2021, 26(23):7177.
[19] Zhuang C, Zhang W, Sheng C, Zhang W, Xing C, Miao Z: Chalcone: A Privileged Structure in Medicinal Chemistry. *Chemical Reviews* 2017, 117(12):7762-7810.
[20] Jung SK, Lee MH, Lim DY, Kim JE, Singh P, Lee SY, et al.: Isoliquiritigenin Induces Apoptosis and Inhibits Xenograft Tumor Growth of Human Lung Cancer Cells By Targeting Both Wild Type and L858R/T790M Mutant EGFR. *Journal of Biological Chemistry* 2014, 289(52):35839-35848.
[21] Aida K, Tawata M, Shindo H, Onaya T, Sasaki H, Yamaguchi T, et al.: Isoliquiritigenin: A New Aldose Reductase Inhibitor From Glycyrrhizae Radix. *Planta Medica* 1990, 56(3):254-258.
[22] Song YQ, Guan XQ, Weng ZM, Liu JL, Chen J, Wang L, et al.: Discovery of hCES2A Inhibitors From Glycyrrhiza Inflata Via Combination of Docking-Based Virtual Screening and Fluorescence-Based Inhibition Assays. *Food & Function* 2021, 12(1):162-176.
[23] Zeng F, Wu W, Zhang Y, Pan X, Duan J: Rapid Screening of Lipase Inhibitors in Licorice Extract by Using Porcine Pancreatic Lipase Immobilized on Fe3O4 Magnetic Nanoparticles. *Food & Function* 2021, 12(12):5650-5657.
[24] Wang Z, Zeng X, Mo Y, Smith K, Guo Y, Lin J: Identification and Characterization of A Bile Salt Hydrolase From Lactobacillus Salivarius for Development of Novel Alternatives to Antibiotic Growth Promoters. *Applied and Environmental Microbiology* 2012, 78(24):8795-8802.
[25] Chand D, Ramasamy S, Suresh CG: A Highly Active Bile Salt Hydrolase From Enterococcus Faecalis Shows Positive Cooperative Kinetics. *Process Biochemistry* 2016, 51(2):263-269.
[26] Brandvold KR, Weaver JM, Whidbey C, Wright AT: A Continuous Fluorescence Assay for Simple Quantification of Bile Salt Hydrolase Activity in the Gut Microbiome. *Scientific Reports* 2019, 9(1):1359.
[27] Tu DZ, Mao X, Zhang F, He RJ, Wu JJ, Wu Y, et al.: Reversible and Irreversible Inhibition of Cytochrome P450 Enzymes by Methylophiopogonanone A. *Drug Metabolism and Disposition* 2020, 49(6):459-469.
[28] He W, Wu JJ, Ning J, Hou J, Xin H, He YQ, et al.: Inhibition of Human Cytochrome P450 Enzymes by Licochalcone A, A Naturally Occurring Constituent of Licorice. *Toxicology In Vitro* 2015, 29(7):1569-1576.
[29] Xin H, Qi XY, Wu JJ, Wang XX, Li Y, Hong JY, et al.: Assessment of the Inhibition Potential of Licochalcone A Against Human UDP-Glucuronosyltransferases. *Food and Chemical Toxicology* 2016, 90:112-122.
[30] Lei W, Wang DD, Dou TY, Hou J, Feng L, Yin H, et al.: Assessment of the Inhibitory Effects of Pyrethroids Against Human Carboxylesterases. *Toxicology and Applied Pharmacology* 2017, 321:48-56.
[31] Huang X, Zhu J, Wang L, Jing H, Ma C, Kou X, et al.: Inhibitory Mechanisms and Interaction of Tangeretin, 5-Demethyltangeretin, Nobiletin, and 5-Demethylnobiletin From Citrus Peels on Pancreatic Lipase: Kinetics, Spectroscopies, and Molecular Dynamics Simulation. *International Journal of Biological Macromolecules* 2020, 164:1927-1938.
[32] Zhou H, Hylemon PB: Bile Acids are Nutrient Signaling Hormones. *Steroids* 2014, 86:62-68.
[33] Fiorucci S, Biagioli M, Zampella A, Distrutti E: Bile Acids Activated Receptors Regulate Innate Immunity. *Frontiers in Immunology* 2018, 9:1853.
[34] Pols TWH, Puchner T, Korkmaz HI, Vos M, Soeters MR, de Vries CJM: Lithocholic Acid Controls Adaptive Immune Responses by Inhibition of Th1 Activation Through the Vitamin D Receptor. *PLoS One* 2017, 12(5):e0176715.
[35] Ridlon JM, Kang DJ, Hylemon PB: Bile Salt Biotransformations By Human Intestinal Bacteria. *Journal of Lipid Research* 2006, 47(2):241-259.
[36] Huang F, Zheng X, Ma X, Jiang R, Zhou W, Zhou S, et al.: Theabrownin From Pu-erh tea Attenuates Hypercholesterolemia Via Modulation of Gut Microbiota and Bile Acid Metabolism. *Nature Communications* 2019, 10(1):4971.

[37] Sun R, Yang N, Kong B, Cao B, Feng D, Yu X, et al.: Orally Administered Berberine Modulates Hepatic Lipid Metabolism by Altering Microbial Bile Acid Metabolism and the Intestinal FXR Signaling Pathway. *Molecular Pharmacology* 2017, 91(2):110-122.

[38] Hua L, Wenyi W, Hongxi X: Drug Discovery is an Eternal Challenge for the Biomedical Sciences. *Acta Materia Medica* 2022, 1(1):1-3.

[39] Batovska DI, Todorova IT: Trends in Utilization of the Pharmacological Potential of Chalcones. *Current Clinical Pharmacology* 2010, 5(1):1-29.

[40] Maria Pia GD, Sara F, Mario F, Lorenza S: Biological Effects of Licochalcones. *Mini-Reviews in Medicinal Chemistry* 2019, 19(8):647-656.

[41] Alam F, Khan GN, Asad M: Psoralea Corylifolia L: Ethnobotanical, Biological, and Chemical Aspects: A Review. *Phytotherapy Research* 2018, 32(4):597-615.

[42] Zhang LL, Tian K, Tang ZH, Chen XJ, Bian ZX, Wang YT, et al.: Phytochemistry and Pharmacology of Carthamus Tinctorius L. *The American Journal of Chinese Medicine* 2016, 44(2):197-226.

[43] Duan J, Dong W, Xie L, Fan S, Xu Y, Li Y: Integrative Proteomics-Metabolomics Strategy Reveals the Mechanism of Hepatotoxicity Induced by Fructus Psoraleae. *Journal of Proteomics* 2020, 221:103767.

[44] Qiao X, Ye M, Xiang C, Bo T, Yang WZ, Liu CF, et al.: Metabolic Regulatory Effects of Licorice: A Bile Acid Metabonomic Study by Liquid Chromatography Coupled with Tandem Mass Spectrometry. *Steroids* 2012, 77(7):745-755.

[45] Jin Y, Wu L, Tang Y, Cao Y, Li S, Shen J, et al.: UFLC-Q-TOF/MS Based Screening and Identification of the Metabolites in Plasma, Bile, Urine and Feces of Normal and Blood Stasis Rats After Oral Administration of Hydroxysafflor Yellow A. *Journal of Chromatography B Analytical Technologies in the Biomedical and Life Sciences* 2016, 1012-1013:124-129.

[46] Sukumaran SD, Chee CF, Viswanathan G, Buckle MJ, Othman R, Abd Rahman N, et al.: Synthesis, Biological Evaluation and Molecular Modelling of 2'-Hydroxychalcones as Acetylcholinesterase Inhibitors. *Molecules* 2016, 21(7).